On the El-Niño Teleconnection to Spring Precipitation in Europe

Geert Jan van Oldenborgh*
Gerrit Burgers
Albert Klein Tank

KNMI, De Bilt, The Netherlands

December 1998
revised July 1999

Abstract
In a statistical analysis of more than a century of data, a strong connection was found between strong warm El Niño winter events and high spring precipitation in a band from southern England eastwards into Asia. This relationship is an extension of the connection mentioned by Kiladis and Diaz (1989), and is much stronger than the winter season teleconnection that has been the subject of other studies. Correlation coefficients between December–February (DJF) NINO3 indices and March–May (MAM) precipitation are higher than $r = 0.3$ for individual stations, and as high as $r = 0.49$ for an index of precipitation anomalies around 50°N from 5°W to 35°E. The lagged correlation suggests that southeast Asian surface temperature anomalies may act as intermediate variables.

1 Introduction

The recent strong El Niño has stirred up again interest in possible teleconnections to Europe. A few influences have been mentioned in previous studies. During the winter season, van Loon and Madden (1981) and Halpert and Ropelewski (1992) found a decrease in temperature and precipitation with El Niño conditions in Scandinavia, in line with Berlage (1966) who noticed that this tends to happen in the year after after cold (La Niña) events. Central

* Correspondence to: KNMI, P. O. Box 201, NL-3730 AE De Bilt, the Netherlands

European winters would have the opposite tendencies, i.e. warmer and wetter (Kiladis and Diaz, 1989) during warm events; this squares with the increase of cyclonic Großwetter days observed in England (Wilby, 1993) and Germany (Fraedrich, 1994) during El Niño years.

For the spring season after an El Niño event, Kiladis and Diaz (1989) note wet precipitation anomalies in central Europe. These are also shown in Moron and Ward (1998), together with strong dry anomalies in eastern Spain; the latter have been studied in Rodo *et al.* (1997). Finally, Halpert and Ropelewski (1992) find cold temperature anomalies in southwestern Europe and northern Africa.

Recently, new data sets of historical data have become available. This has opened up the possibility to check existing conjectures at higher statistical significance levels. The present study was initiated by a search for an ENSO influence in The Netherlands through tropical storm activity. Tropical storm and hurricane activity on the Atlantic is suppressed by El Niño (Gray, 1984), and many catastrophic downpours in De Bilt are remnants of tropical storms during the Atlantic hurricane season. However, this does not lead to an observable anti-correlation between the NINO3 index and precipitation (or high-precipitation events).

In this article a new analysis is presented of the strongest statistical connection that was found between ENSO and the weather in Europe: increased spring precipitation after an El Niño event. In section 2 the connection for one station, De Bilt in the Netherlands, is detailed. The relationship is extended over Europe in section 3, and possible mechanisms are discussed in section 4.

2 Rain in De Bilt

Two years ago we noticed that there was a correlation between the strength of an El Niño, quantified by the NINO3.4 index[1] and spring (March–May, MAM) precipitation in De Bilt (central Netherlands) using data from 1950 to 1995. With a 3-month lag the correlation coefficient was 0.30, with a nominal significance of 95%. Given that more than 24 possible relationships had been considered, this result was not very convincing. It hinged on one extreme event: in

1. the NINO3.4 index is the average sea surface temperature (SST) in the region 5°S–5°N, 120°W–170°W, the values where obtained from the U. S. National Centers for Environmental Prediction (NCEP); (Reynolds and Smith, 1994).

1983 the spring had been extraordinarily wet (see figure 1). Recently the the precipitation series was extended back to 1849 and forward to 1998[2] including a few more strong El Niño events. In addition, Kaplan *et al.* (1998) provide a reconstruction of the NINO3 index[3] from 1856 to 1991. The series uses only SST measurements, and correlates quite well with the Jakarta Southern Oscillation index (SOI) of Können *et al.* (1998): $r = 0.66$ in December–February (DJF) and 0.67 in MAM over 133 years in 1859–1996. From 1950 onwards the NCEP analyses are used (Reynolds and Smith, 1994), over the overlap period the correlation with the Kaplan NINO3 is 0.97. An analysis using the standard SOI (Allan *et al.*, 1991; Können *et al.*, 1998) yields essentially the same results.

Figure 1 shows that the relationship between the winter (DJF) NINO3 index and spring (MAM) precipitation in De Bilt was confirmed in the new analysis. The correlation coefficient is $r = 0.35$; nominally there is a chance $p < 10^{-4}$ that this is the result of a random fluctuation of uncorrelated data (two-sided t-test). The average of the four Dutch stations with data from 1867 (De Bilt, Groningen, Den Helder and Hoofddorp) gives a correlation of 0.40.

To quantify the significance of these relationships, the data were divided into two groups, one with NINO3 index $N_3 < N_3^{cut}$ and one with $N_3 > N_3^{cut}$. This was carried out for different values of N_3^{cut}. For the De Bilt data, the averages and the two-sigma bands of the NINO3 index distributions of the two groups are shown in figure 2 as a function of the cut-off value N_3^{cut}. According to a non-parametric Kolmogorov-Smirnov test, the difference between the two distributions is significant at the 99% level if $N_3^{cut} > 0.5$: El Niño years have a tendency to be followed by wetter springs than other years. On the other hand, the difference between La Niña years and the complement is not significant for the De Bilt data, even at the 95% level. For the four-station average this asymmetry between El Niño and La Niña is less pronounced (not shown), here the difference between the two distributions is significant at the 95% level if $N_3^{cut} < -0.5$.

The signal has no connection with the North Atlantic Oscillation (NAO). On the one hand the NAO does not influence spring precipitation in The Netherlands very much ($r = -0.01$) while, on the other hand ENSO and NAO are only correlated in the summer over the last century, and not in the spring ($r = -0.09$ in MAM).

---

2. the series is available upon request from the KNMI.

3. the NINO3 index is the average sea surface temperature in the region 5°S–5°N, 90°W–150°W.

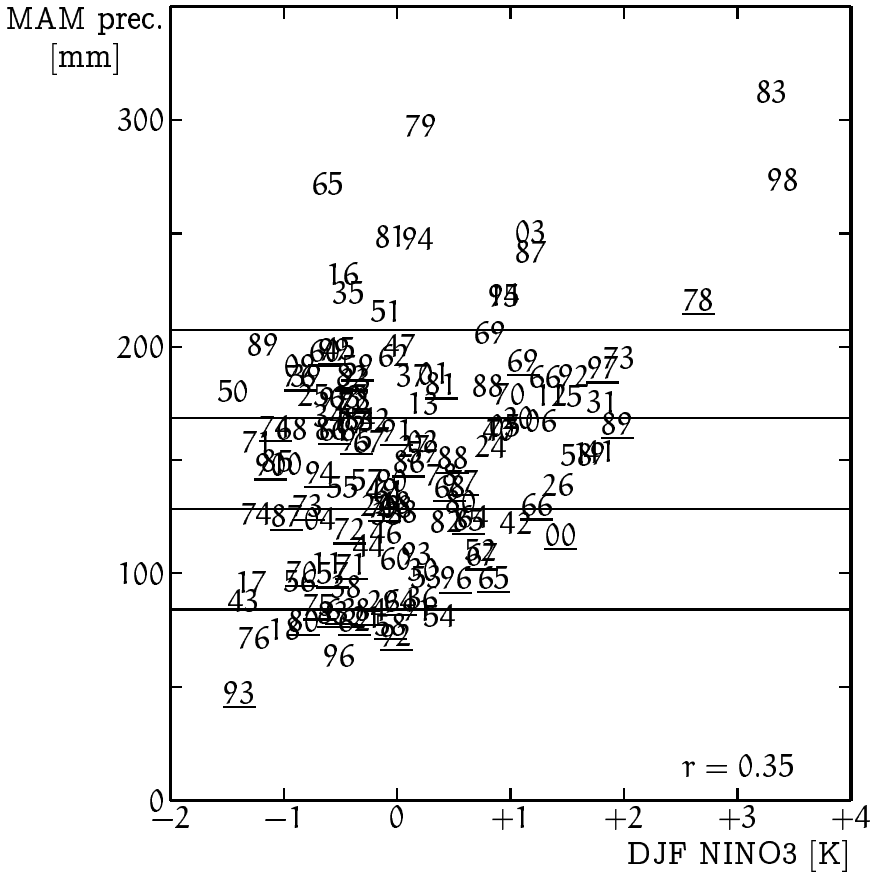

Figure 1: A scatter plot of spring (MAM) precipitation in De Bilt, Netherlands versus the previous winter NINO3 index of SST in the eastern Pacific for 1857–1998. Underlined numbers refer to the 19th century. The horizontal thin lines give the 10%, 33%, 67% and 90% percentiles.

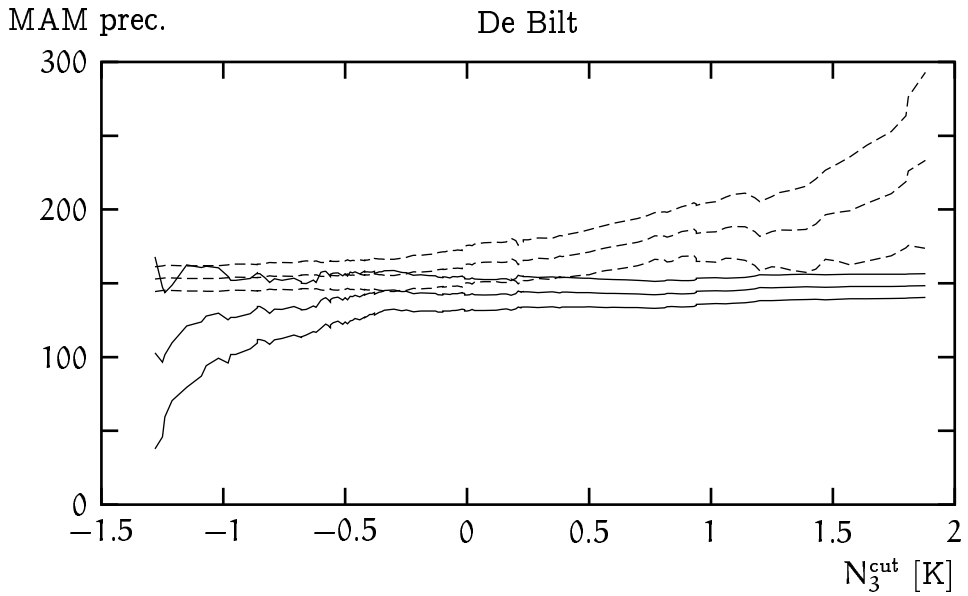

Figure 2: Mean and two-sigma uncertainties of the precipitation in De Bilt for the years with $N_3 > N_3^{cut}$ (dashed curves), and $N_3 < N_3^{cut}$ (solid curves).

3 Spring rain in Europe

We investigated the extent of the teleconnection using the U. S. Natonal Climate Data Center gridded precipitation anomalies database (Baker *et al.*, 1995). This contains global data from 1851 to 1993 in $5^\circ \times 5^\circ$ bins. In figure 3 one sees that the spring precipitation increases after an El Niño in a zonal belt from England and France to the Ukraine, with a weaker extension eastwards into Asia. There are two maxmima, with correlations coefficients above 0.3 (without the 1998 El Niño): one over southern England, northern France, the Low Countries and Germany, and another one in the Ukraine centered on Kiev ($r = 0.43$). This last point was also noted by Kiladis and Diaz (1989). In their figure 3h a similar but more southerly band is indicated over Europe. This band forms a dipole with the drier zone over Northern Africa and eastern Spain ($r = -0.35$), which was also noted in Kiladis and Diaz (1989) and studied in Rodo *et al.* (1997). In contrast, the correlation of DJF precipitation with the DJF NINO3 index only reaches values above 0.2 in three grid points: 0.22 in Brussels, 0.23 in Moscow and −0.29 in Bergen, Norway; none of these reach 99% levels of significance. The Iberian signals in the summer and early autumn are also weaker (not shown).

The relation with ENSO is seen more clearly with the construction of

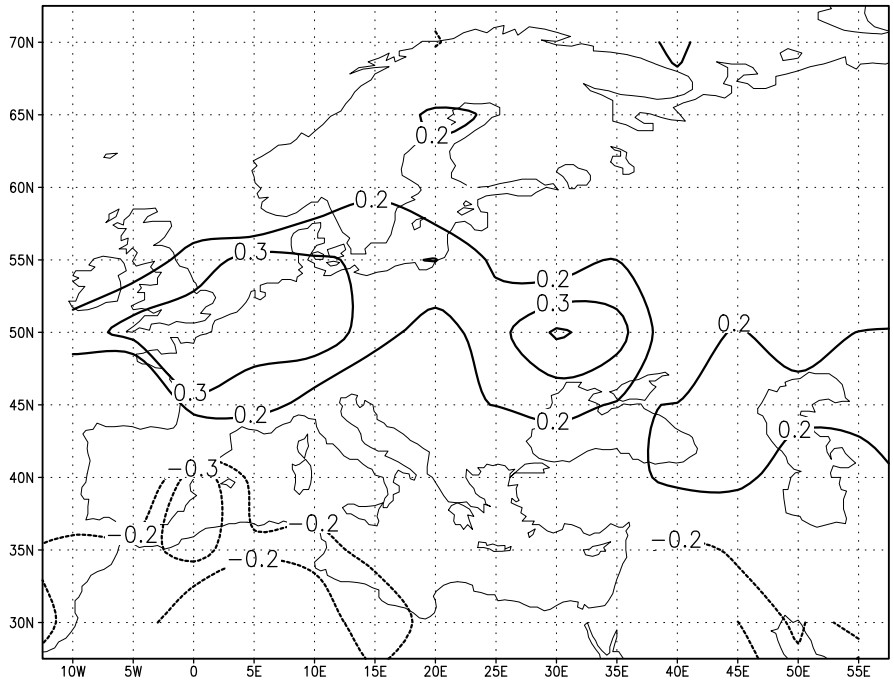

Figure 3: The correlation coefficients of the DJF NINO3 index and the MAM precipitation over Europe (1857–1993).

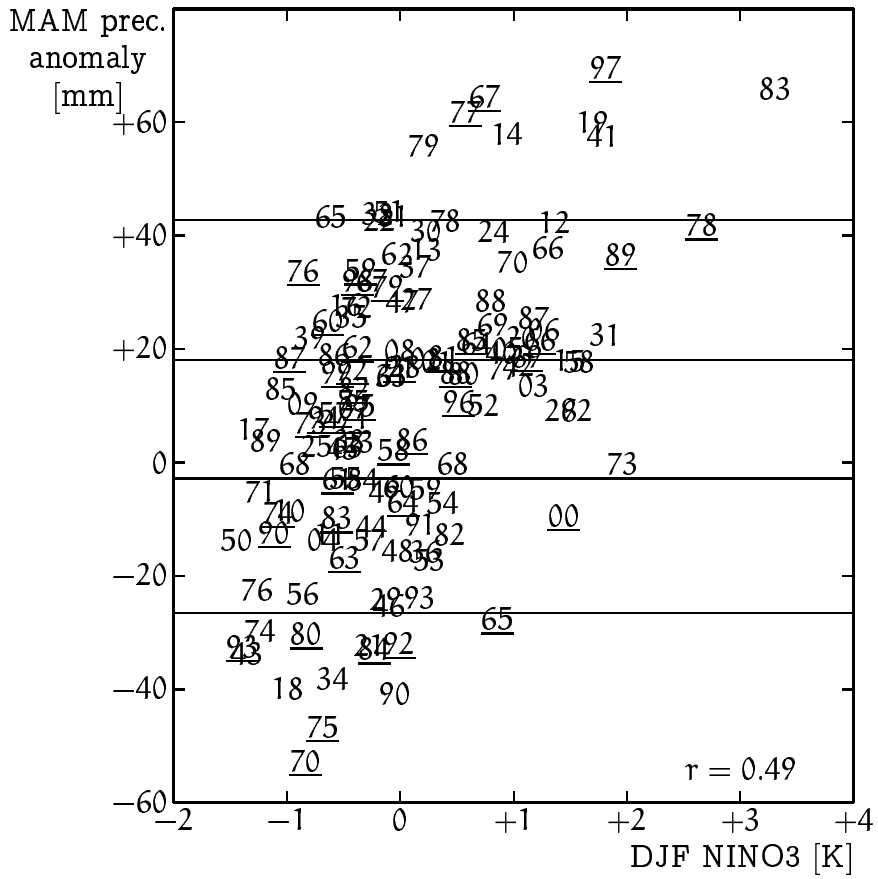

Figure 4: Scatter plot of the MAM precipitation anomalies in Europe around 50°N against the DJF NINO3 index for 1857–1993.

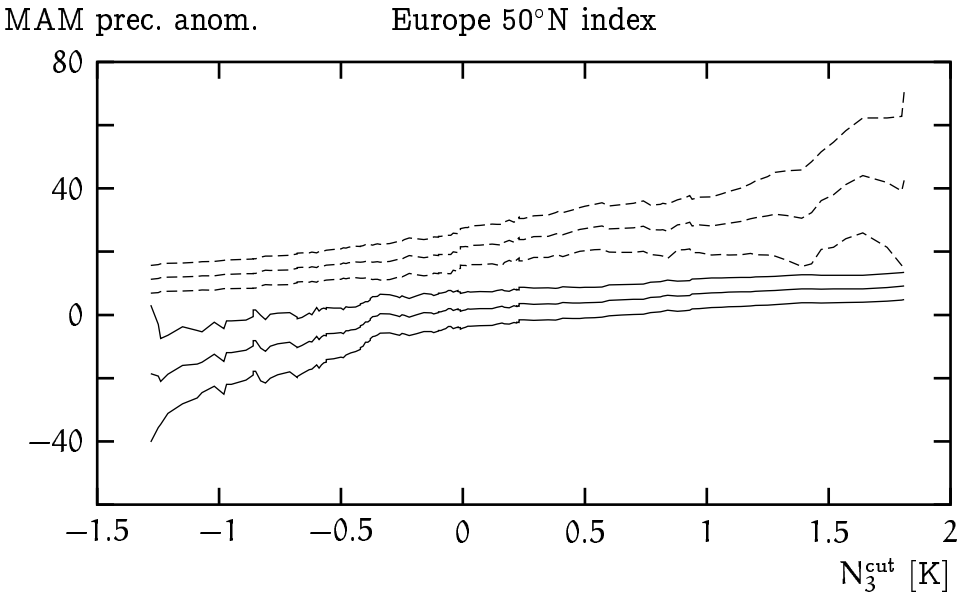

Figure 5: Mean and two-sigma uncertainties of the precipitation anomaly around 50°N from 5°W to 35°E. Dashed curves: the years with $N_3 > N_3^{cut}$, solid curves: below $N_3 < N_3^{cut}$.

an index of average MAM rainfall anomalies over the band with positive correlations consisting of nine $5° \times 5°$ grid boxes centered on 50°N from 5°W to 35°E. This index has a correlation coefficient $r = 0.49$ with DJF NINO3. It can be seen from figure 5 that the difference between years with NINO3 index $N_3 < N_3 3^{cut}$ and years with $N_3 > N_3^{cut}$ looks significant for the entire range of cut-off values N_3^{cut}. A Kolmogorov-Smirnov test confirms that the distribution of years with $N_3 < N_3^{cut}$ and that of years with $N_3 > N_3^{cut}$ are different at the 99% level for all choices of N_3^{cut}.

The correlation with the NAO is again low, although non-zero ($r = -0.16$). The dipole pattern in figure 3 is very different from the NAO pattern, which has a positive maximum between western Norway, Iceland and Scotland, and negative minima over the south-western Iberian peninsula and the Black Sea. Also, the ENSO pressure teleconnection (figure 7b) is located over Europe, not over the Atlantic Ocean. It is therefore treated as a distinct mode.

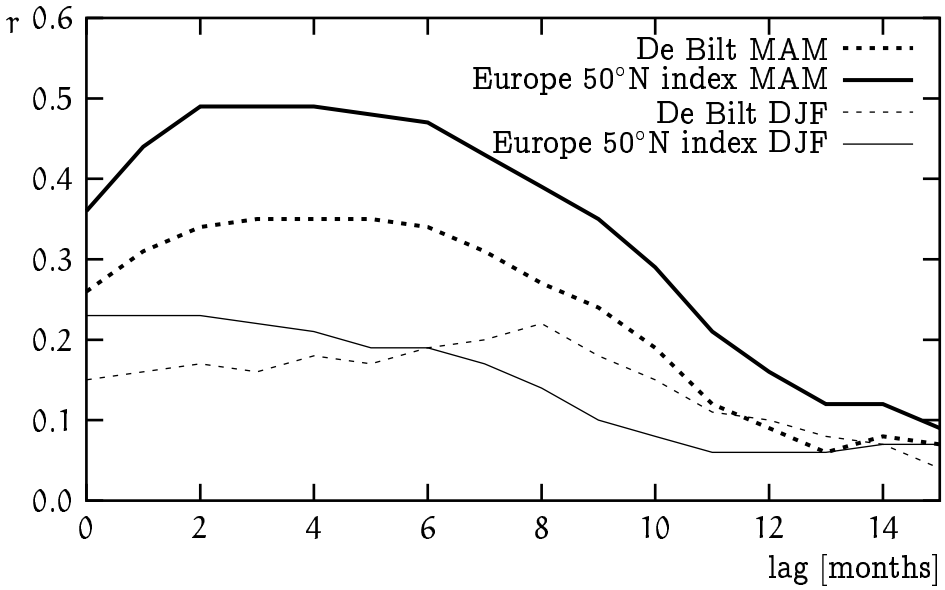

Figure 6: Lag correlation coefficients of the precipitation in spring and winter in De Bilt and in Europe around 50°N with the NINO3 index.

4 Possible mechanisms

Possible mechanisms of this teleconnection must explain the time structure of the correlation. The lag correlations of the MAM precipitation with the NINO3 index are shown in figure 6. For reference the DJF correlations are also shown. Although there is room for an atmospheric mechanism with a time scale shorter than a month, the main signal seems to be delayed by 3–6 months. This agrees with the observation that the correlations of the MAM NINO3 index with historical sea level pressure data (1873–1995, Jones, 1987; Basnett and Parker, 1997) are not very high, although they are significant. In Fig. 7a it can be seen that, in a band from the British Isles to the Ukraine, sea-level pressure tends to be lower during El-Niño events. The correlation coefficient r just reaches -0.20 ($p = 97\%$) over the North Sea and -0.16 in the Ukraine ($p = 92\%$). It is, on average, somewhat higher in Northern Africa: $r = 0.23$ at the Straits of Gibraltar ($p = 99\%$). This is the correct structure to explain more rain in the dipole of figure 3. The lag-3 signal (Fig. 7b) has the same features, but is stronger: $r = -0.26$ over the North Sea, 0.27 at Gibraltar.

The 3–6 month delay points at the possibility that, in addition to this direct teleconnection, there is an intermediate variable—probably SST in a third

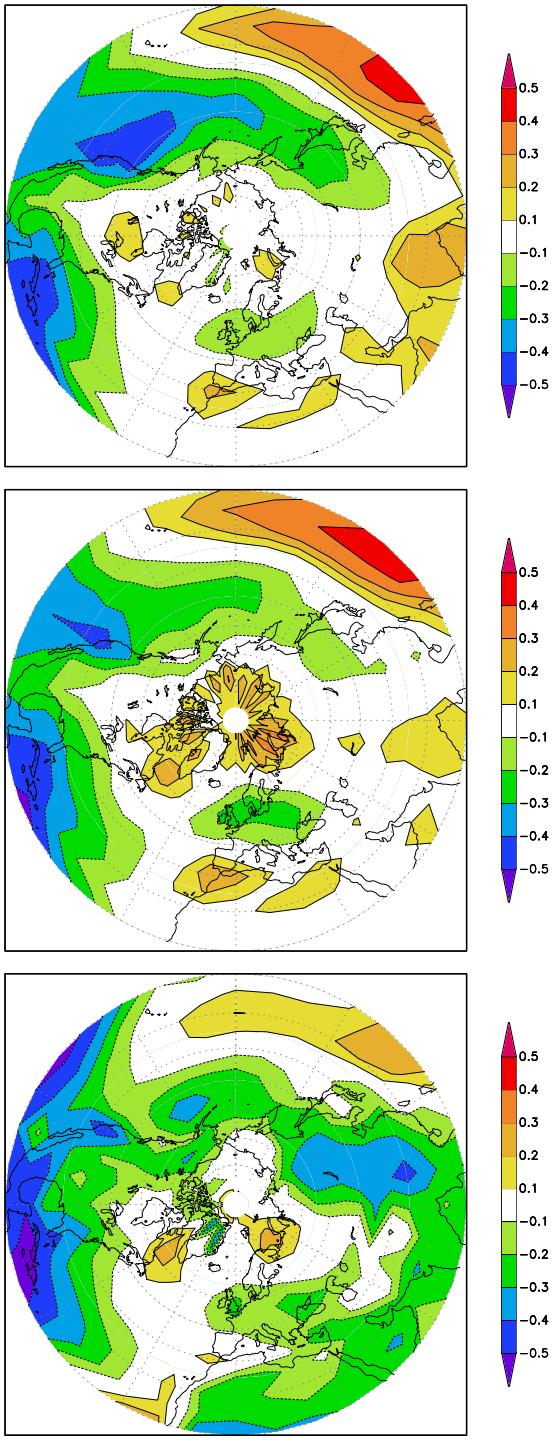

Figure 7: Correlation maps of MAM northern hemisphere sea level pressure (1873-1995) and (a) MAM NINO3, (b) DJF NINO3, and (c) an index of SE Asia SST.

		NINO3.4	SE Asia	N Pacific	Atlantic	De Bilt	50°N
DJF	NINO3	0.80	0.67	0.49	0.43	0.35	0.49
MAM	NINO3.4	1.00	0.67	0.50	0.35	0.22	0.28
	SE Asia		1.00	0.47	0.56	0.36	0.35
	N Pacific			1.00	0.31	0.26	0.30
	Atlantic				1.00	0.35	0.27
	De Bilt					1.00	0.60
	50°N						1.00

Table 1: Correlation coefficients between the DJF Kaplan/NCEP NINO3 index; the MAM NINO3.4, SE Asia, North Pacific and subtropical Atlantic temperature indices extracted from Parker *et al.* (1995); and MAM De Bilt and European 50°N precipitation.

region—that is influenced by ENSO and in turn causes more rain around 50°N in Europe in spring. To investigate this, the historical temperature anomalies database of Jones and Parker (Parker *et al.*, 1995; Jones, 1994; Parker *et al.*, 1994) is used, which includes SST as well as land 2 m temperatures. In Fig. 8 (top panel), the correlation of these temperatures with the European 50°N spring precipitation index is shown. Locally, high precipitation is associated with colder water in the northeast Atlantic. One also recognizes the NAO SST signature in the west Atlantic, in spite of the low correlation with the atmospheric NAO index. However, both of these patterns are only very weakly associated with ENSO, as can be seen from the middle panel in which the correlations of this MAM temperature field and the DJF NINO3 index are shown.

The overlap between these two plots is shown in the bottom panel, in which the product of the top two panels is plotted, $r^{lag3}_{NINO3,SST} \times r_{SST,P(50°N)}$. If only one area would act as intermediate variable the local value would be equal to $r^{lag3}_{NINO3,P(50°N)} = 0.49$. Even if more intermediate variables contribute, areas in which both correlations are high will stand out in this plot, but a quantitative interpretation cannot be given. It can be seen that none of the regions reach values as high as 0.49, but there are four areas of possible interest: the central equatorial Pacific, Southeast Asia and parts of the Indian Ocean, the North Pacific dipole and the subtropical Atlantic.

We defined four temperature anomaly indices corresponding to these regions from the Jones and Parker dataset including both sea and land points.

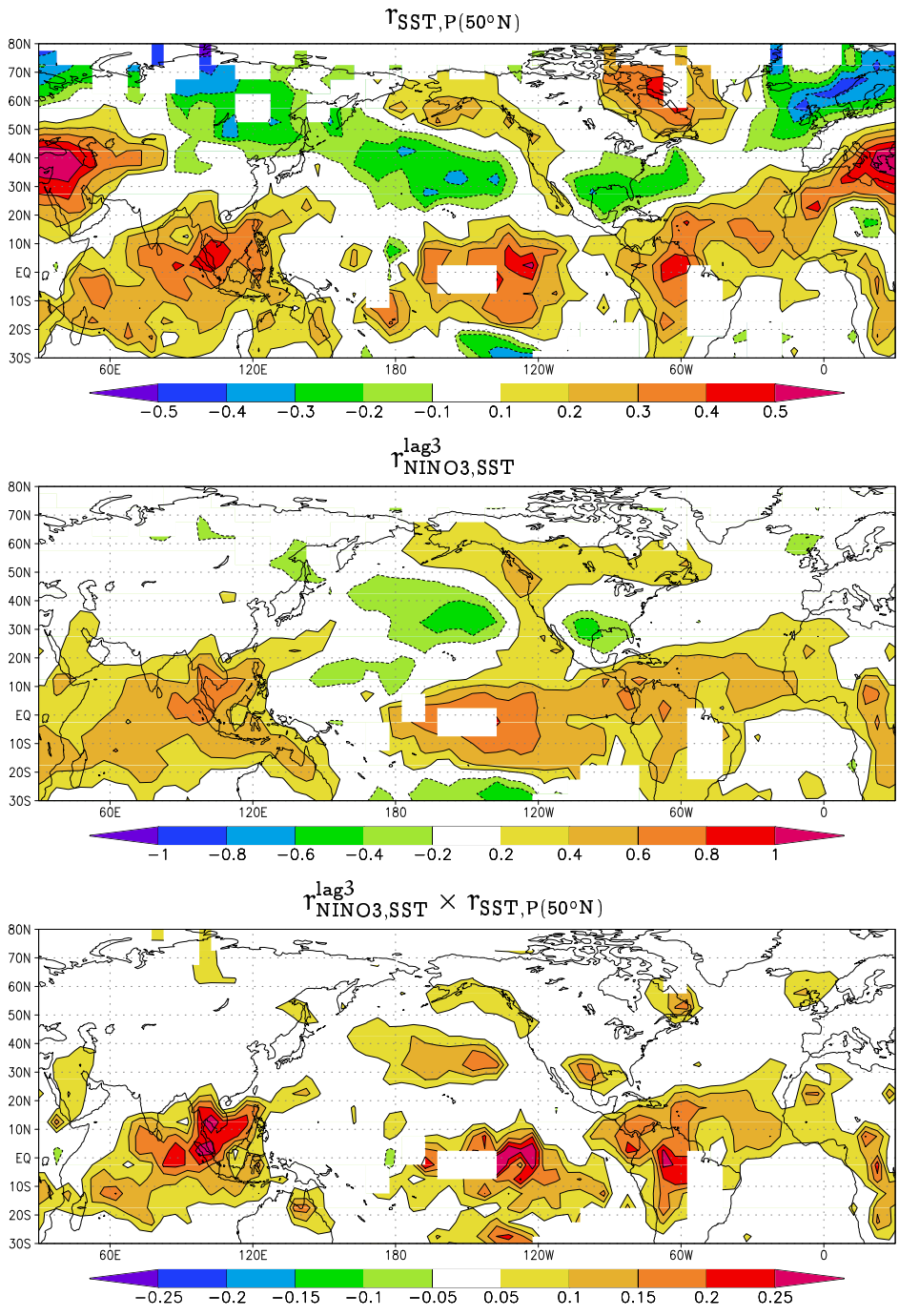

Figure 8: The correlation of spring precipitation around 50°N in Europe with the Jones and Parker temperature dataset (top), the lag-3 correlation of this temperature and the NINO3 index (middle) and the product of the these two correlations (bottom). Note the different scales.

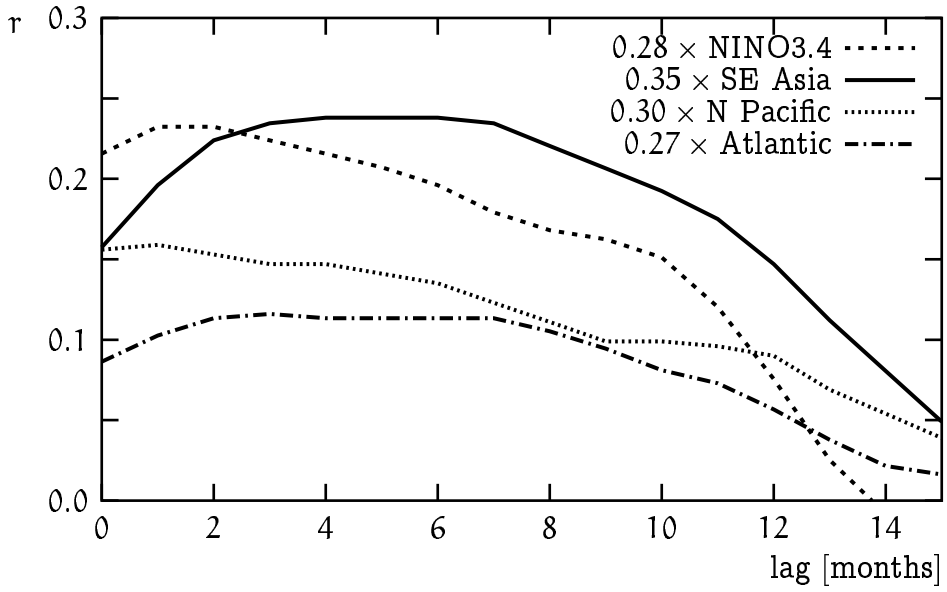

Figure 9: Lag correlation coefficients of the MAM temperature anomalies in the four possible source regions with the NINO3 index, weighted with the correlation coefficients with the Europe 50°N precipitation index in spring.

For the Central Pacific we use the NINO3.4 region, for south-east Asia the box 60°E – 120°E, 10°S – 20°N, for the North Pacific dipole the region 160°E – 120°W, 30°N – 60°N with a top-left/bottom-right dipole structure and finally for the subtropical Atlantic the box 20°W – 70°W, EQ – 25°N. The correlation coefficients between all these indices are given in table 1. In figure 9 the lag-correlation coefficients of these indices with the NINO3 index are plotted, multiplied by their correlation with the European 50°N spring precipitation index. It can be seen that the shape of the lag structure of the south-east Asian region corresponds closely to the observed signal. Also the signal in pressure (Fig. 7c) is very similar to the lagged NINO3 signal over Europe (Fig. 7b), but the North African opposite-sign anomaly has disappeared. However, the correlation of the Southeast Asia index with rainfall in Europe is only 0.35, which is lower than the lagged correlation with NINO3 instead of the higher value expected for an intermediate variable. This could partly be a result of other mechanisms, such as the direct link from the central Pacific, but the nature of the measurements also plays a role. Temperature differences in the south-east Asia area are small: the MAM variance is only $(0.28\,\mathrm{K})^2$, which is much less than the $(0.88\,\mathrm{K})^2$ of the DJF NINO3 index. This increases the effect of noise in

the form of measurement errors, irrelevant land points and small-scale weather. On the basis of the time delays of the signal it can be concluded that Southeast Asia is most likely the main source of the influence of ENSO on the weather of Europe, with a smaller direct link from the central Pacific.

The importance of the Southeast Asia SST for the northern hemisphere circulation is supported by data analyses and modelling studies, see for example the review by Trenberth *et al.* (1998). In spring the most active teleconnection is the North Pacific pattern. This corresponds to the top halves of Figure 7a,b. The lower halves show an extension across the North Pole into Europe. This extension substantiates arguments using simplified Rossby wave propagation. Unfortunately, virtually all modelling studies have been conducted for northern winter conditions, when the observations contain a much weaker teleconnection. Still, indications of the pole-crossing response can be seen in DJF atmosphere general circulation model results (see, for example, Ferranti *et al.*, 1994). It can be speculated that the spring transition to the Asian and Chinese monsoon systems makes the circulation more susceptible to perturbations. Further modelling work is clearly needed in order to elucidate the mechanism behind the teleconnection to Europe.

5 Conclusions

Using more than a century of data, a clear influence of ENSO on the weather in Europe has been established: spring precipitation in a belt around 50°N from southern England to the Ukraine tends to increase after an El Niño and to decrease after a La Niña. The strength of the correlation is $r = 0.49$ for an index of precipitation in this belt, $r = 0.40$ for the average of four Dutch stations, and $r = 0.35$ for the single station at De Bilt. Other European ENSO teleconnections are weaker than this. The 3-6 month lag and correlation maps suggest that Southeast Asian surface temperatures may act as an intermediate variables for most of the signal.

Acknowledgements We would like to thank Theo Opsteegh and Robert Mureau for many useful discussions.

References

Allan, R. J., Nicholls, N., Jones, P. D., and Butterworth, I. J. 1991. 'A further extension of the Tahiti-Darwin SOI, early SOI results and Darwin pressure', *J. Climate,* **4**, 743–749. The series can be found at http://www.cru.uea.ac.uk/cru/data/soi.htm.

Baker, C. B., Eischeid, J. K., Karl, T. R., and Diaz, H. F. 1995. 'The quality control of long-term climatological data using objective data analysis', in *Preprints of AMS Ninth Conference on Applied Climatology* Dallas TX, January 15–20 1995. American Meteorological Society, Boston, MA. The data are available from http://www.ncdc.noaa.gov/onlinedata/climatedata/grid.prcp.seasanom.html.

Basnett, T. A. and Parker, D. E. 1997. 'Development of the global mean sea level pressure data set GMSLP2', Climatic Research Technical Note 79 Hadley Centre Meteorological Office, Bracknell, U. K. 16pp plus Appendices. Data are available from http://www.cru.uea.ac.uk/cru/data/pressure.htm.

Berlage, H. P. 1966. *The Southern Oscillation and World Weather* Number 88 in Mededelingen en verhandelingen. KNMI 152 pp.

Ferranti, L., Molteni, F., and Palmer, N. 1994. 'Impact of localized tropical and extratropical SST anomalies in ensembles of seasonal GCM integrations', *Quart. J. Roy. Meteorol. Soc.,* **120**, 1613–1645.

Fraedrich, K. 1994. 'An ENSO impacty on Europe?', *Tellus,* **46A**, 541–552.

Gray, W. M. 1984. 'Atlantic seasonal hurricane frequency: Part I: El Niño and 30 mb quasi–biennial oscillation influences', *Mon. Wea. Rev.,* **112**, 1649–1668.

Halpert, M. S. and Ropelewski, C. F. 1992. 'Surface temperature patterns associated with the Southern Oscillation', *J. Climate,* **5**, 577–593.

Jones, P. D. 1987. 'The early twentieth century arctic high — fact or fiction?', *Climate Dynamics,* **1**, 63–75.

Jones, P. D. 1994. 'Hemispheric surface air temperature variations: a reanalysis and an update to 1993', *J. Climate,* **7**, 1794–1802.

Kaplan, A., Cane, M. A., Kushnir, Y., Clement, A. C., Blumenthal, M. B., and Rajagopalan, B. 1998. 'Analyses of global sea surface temperature 1856–1991', *J. Geophys. Res.,* **103**, 18567–18589. Data are available from http://ingrid.ldgo.columbia.edu.

Kiladis, G. N. and Diaz, H. F. 1989. 'Global climatic anomalies associated with extremes in the southern oscillation', *J. Climate,* **2**, 1069–1090.

Können, G. P., Jones, P. D., Kaltofen, M. H., and Allan, R. J. 1998. 'Pre-

1866 extensions of the Southern Oscillations index using early Indonesian and Tahitian meteorological readings', *J. Climate,* **11**, 2325–2339.

Moron, V. and Ward, M. N. 1998. 'ENSO teleconnections with climate variability in the European and African sector', *Weather,* **53**, 287–295.

Parker, D. E., Folland, C. K., and Jackson, M. 1995. 'Marine surface temperature: observed variations and data requirements', *Climatic Change,* **31**, 559–600.

Parker, D. E., Jones, P. D., Bevan, A., and Folland, C. K. 1994. 'Interdecadal changes of surface temperature since the late 19th century', *J. Geophys. Res.,* **99**, 14373–14399. Data are available from http://www.cru.uea.ac.uk/cru/data/temperat.htm.

Reynolds, R. W. and Smith, T. M. 1994. 'Improved global sea surface analyses using optimum interpolation', *J. Clim.,* **7**, 929–948. NINO indices are available from the Climate Prediction Center at http://nic.fb4.noaa.gov/data/cddb/altindex.html.

Rodo, X., Baert, E., and Comin, F. A. 1997. 'Variations in seasonal rainfall in Southern Europe during the present century: relationships with the North Atlantic Oscillation and the El Niño–Southern Oscillation', *Climate Dynamics,* **13**, 275–284.

Trenberth, K. E., Branstator, G. W., Karoly, D., Kumar, A., Lau, N.-C., and Ropelewski, C. 1998. 'Progress during TOGA in understanding and modeling global teleconnections associated with tropical sea surface temperatures', *J. Geophys. Res.,* **103**, 14291–14324.

van Loon, H. and Madden, R. A. 1981. 'The Southern Oscillation, Part I. Global associations with pressure and temperature in northern winter', *Mon. Wea. Rev.,* **109**, 1150–1162.

Wilby, R. 1993. 'Evidence of ENSO in the synoptic climate of the British Isles since 1880', *Weather,* **48**, 234–239.